Hexalacunary [α-H₂P₂W₁₂O₄₈]¹²⁻ Wells-Dawson Anion: X-ray Crystal Structure Evidence and Oligomerization to WO(OH₂)⁴⁺-Bridged Dimer and Trimer

Sugiarto[a] and Masahiro Sadakane*[a]

[a]   Dr. Sugiarto, Prof. Dr. M. Sadakane
        Department of Applied Chemistry, Graduate School of Advanced Science and Engineering, Hiroshima University
        1-4-1 Kagamiyama, Higashi-Hiroshima 739-8527, Japan
        E-mail: sadakane09@hiroshima-u.ac.jp
        Homepage: https://catalche.hiroshima-u.ac.jp

        Supporting Information for this article is provided via a link at the end of the document.

Abstract: We report the first single-crystal X-ray structure evidence of the potassium salt of the hexalacunary $[\alpha\text{-H}_2\text{P}_2\text{W}_{12}\text{O}_{48}]^{12-}$ (abbreviated as $\{\text{P}_2\text{W}_{12}\}$) anion after its discovery by Contant and Ciabrini in 1977. In addition, we observed oligomerization of $\{\text{P}_2\text{W}_{12}\}$ into a $\{\text{WO(OH}_2)\}^{4+}$-bridged Pacman-shaped $[\{\text{WO(OH}_2)\}(\alpha\text{-HP}_2\text{W}_{12}\text{O}_{48})_2]^{22-}$ ($\{\text{P}_4\text{W}_{25}\}$) dimer and a cyclic $[\{\text{WO(OH}_2)\}_3(\text{P}_2\text{W}_{12}\text{O}_{48})_3]^{30-}$ ($\{\text{P}_6\text{W}_{39}\}$) trimer. The three phosphotungstate anions were synthesized through recrystallization of $(\text{NH}_4)_{12}[\alpha\text{-H}_2\text{P}_2\text{W}_{12}\text{O}_{48}]$ from slightly alkaline $(\text{HOCH}_2)_3\text{CNH}_2/\text{KCl}$, $\text{CH}_3\text{NH}_3\text{Cl/KCl}$, and $\text{CH}_3\text{NH}_3\text{Cl/NH}_4\text{Cl}$ solutions. The structure of $\{\text{P}_2\text{W}_{12}\}$ is derived from $[\alpha\text{-P}_2\text{W}_{18}\text{O}_{62}]^{6-}$ that has six tungsten—one from each polar group and four from the belt—removed, and the center of the lacunary site is capped by a potassium cation. Structures of $\{\text{P}_4\text{W}_{25}\}$ and $\{\text{P}_6\text{W}_{39}\}$ are constructed by connecting two and three $\{\text{P}_2\text{W}_{12}\}$ units with $\{\text{WO(OH}_2)\}^{4+}$, respectively. The isolation of a pure $\{\text{P}_6\text{W}_{39}\}$ phosphotungstate framework without coordination with transition metal cations is unprecedented. Powder X-ray diffraction confirmed the bulk purity of these compounds, indicating that selective crystallization was achieved through the selection of countercations and pH.

Introduction

Polyoxometalate anions are molecular metal oxides of group 5 (V, Nb, and Ta) and 6 (Mo and W) elements, which have garnered considerable attention because of their rich structures and properties that are applicable in diverse research areas such as catalysis,[1] proton conductivity,[2] molecular magnetism,[3] and biology.[4] In particular, phosphate-containing polyoxotungstates (or phosphotungstates), such as the well-known Keggin $[\text{PW}_{12}\text{O}_{40}]^{3-}$ and Wells-Dawson $[\text{P}_2\text{W}_{18}\text{O}_{62}]^{6-}$, are vital species owing to their ability to remove one or several $\{\text{WO}_x\}$ units from their tungsten-oxygen framework, forming a group of lacunary or defect phosphotungstates. These defect clusters contain highly nucleophilic oxygen atoms, making them attractive building blocks for the synthesis of diverse families of mixed-metal phosphotungstate clusters.[5]

The hexalacunary Wells-Dawson $[\alpha\text{-H}_2\text{P}_2\text{W}_{12}\text{O}_{48}]^{12-}$ anion ($\{\text{P}_2\text{W}_{12}\}$) is a hydrolysis product of $[\text{P}_2\text{W}_{18}\text{O}_{62}]^{6-}$ in $(\text{HOCH}_2)_3\text{CNH}_2/\text{K}_2\text{CO}_3$ solution[6] and it was first reported by Contant and Ciabrini in 1977 as a potassium salt.[7] At that time, the structure of $\{\text{P}_2\text{W}_{12}\}$ was thought to be derived from $[\alpha\text{-}$

$\text{P}_2\text{W}_{18}\text{O}_{62}]^{6-}$ by removing six tungsten atoms occupying the polar caps (the anion was formulated as $[\text{H}_6\text{P}_2\text{W}_{12}\text{O}_{50}]^{12-}$).[7] However, a ^{183}W NMR study[8] on $[\text{P}_2\text{Mo}_6\text{W}_{12}\text{O}_{62}]^{6-}$ by Baker et al. in 1984 indicated that $\{\text{P}_2\text{W}_{12}\}$ has a boat-shaped structure obtained by peeling off a longitudinal third (referred to as "W_6O_{14}" fragment) from a $[\alpha\text{-P}_2\text{W}_{18}\text{O}_{62}]^{6-}$ anion, as illustrated in Scheme 1. Since then, $\{\text{P}_2\text{W}_{12}\}$ has been a vital precursor in the preparation of chiral $[\alpha_1\text{-P}_2\text{W}_{17}\text{O}_{61}]^{10-}$ anion[6, 9] and various multi-metal-containing polyoxotungstates such as $[\text{P}_2\text{W}_{12}\{\text{Nb(O}_2)\}_6\text{O}_{56}]^{6-}$,[10] $[\text{P}_2\text{W}_{12}\text{V}_6\text{O}_{62}]^{12-}$,[11] $[\text{H}_4\text{P}_2\text{W}_{12}\text{Fe}_9\text{O}_{56}(\text{acetate})_7]^{6-}$,[12] $[\text{H}_{55}(\text{P}_2\text{W}_{12}\text{O}_{48})_4\text{WFe}_{27}\text{O}_{56}]^{26-}$,[12] $[\text{H}_{31}(\text{P}_2\text{W}_{12}\text{Nb}_6\text{O}_{62})_6\text{Mn}_{15}\text{Na(OH)}_{12}]^{10-}$,[13] $[(\text{P}_2\text{W}_{12}\text{Nb}_7\text{O}_{63}(\text{OH}_2)_2)_4\text{Nb}_4\text{O}_4(\text{OH})_6]^{30-}$,[14] V-shaped dimer derivatives such as $[\{\text{Co(OH}_2)_4\}\text{P}_4\text{W}_{24}\text{O}_{92}(\text{POC}_6\text{H}_5)_2]^{14-}$,[15] $[\text{Na}\{\text{Ln(H}_2\text{O)}\}\{\text{WO(H}_2\text{O)}\}\text{P}_4\text{W}_{26}\text{O}_{98}]^{12-}$,[16] $[(\text{H}_2\text{P}_4\text{W}_{24}\text{O}_{92})_2(\text{SnMe}_2)_4]^{28-}$,[17] and $[\text{P}_2\text{W}_{24}\text{O}_{92}\text{W}_2\text{O}_8\text{Co}_2]^{20-}$;[18] trimers such as cyclic $[(\text{P}_2\text{W}_{12}\text{O}_{48})_3\{\text{WO(OH}_2)\}_3(\text{guest-transition-metals})]^{n-}$ in which guest-transition-metals are V, Mn, Ni, Co, or Cu[19] and U-shaped $[\text{Li(H}_2\text{O)K}_4(\text{H}_2\text{O})_3\{(\text{UO}_2)_4(\text{O}_2)_4\text{-}(\text{H}_2\text{O})_2\}_2(\text{PO}_3\text{OH})_2\text{P}_6\text{W}_{36}\text{O}_{136}]^{25-}$;[20] cyclic tetramers such as superlacunary $[\text{P}_8\text{W}_{48}\text{O}_{184}]^{40-}$[21] and $[\{\gamma\text{-P}_2\text{W}_{12}\text{O}_{48}\text{Mn}_4(\text{H}_2\text{O})_6\}_4(\text{H}_2\text{O})_4]^{24-}$;[22] and a cyclic hexamer $[\{\text{P}_2\text{W}_{12}\text{O}_{48}\text{Mn}_4(\text{acetylacetonate})_2(\text{acetate})\}_6]^{42-}$;[22] selected clusters are depicted in Scheme 1c.
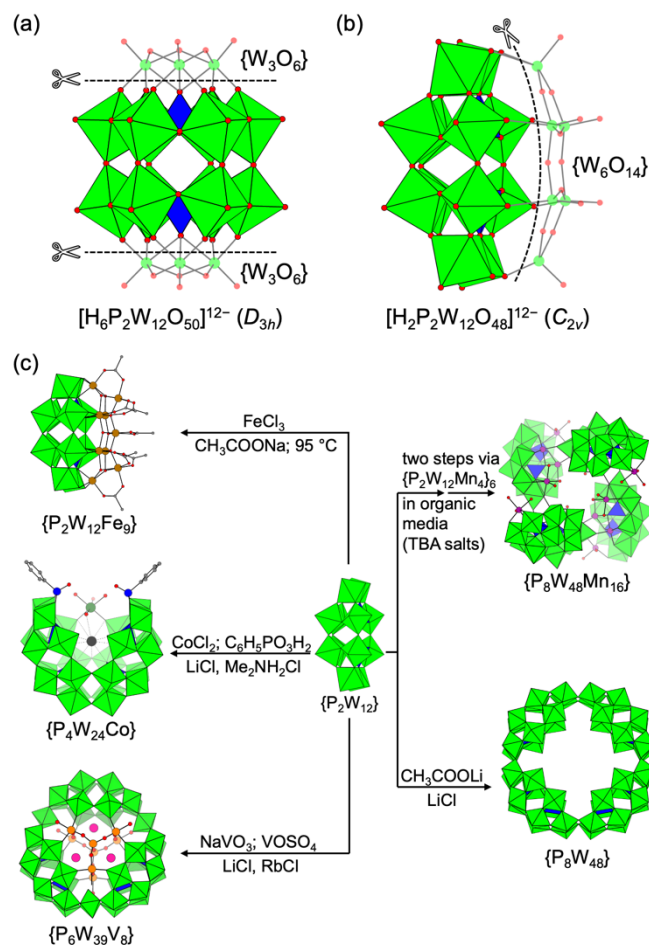
Scheme 1. Structure of {P2W12} (a) proposed by Contant and Ciabrini in 1977 and (b) based on 183W NMR study on [P2Mo6W12O62]6− by Baker's group in 1984. (c) {P2W12} as a gateway to access multi-metallic polyoxotungstate clusters. Color scheme: gray, C; red, O; blue, P; black, K; orange, V; magenta, Rb; purple, Mn; brown, Fe; deep green, Co; green, W. Abbreviations: {P2W12Fe9} = [H4P2W12Fe9O56(acetate)7]6−; {P4W24Co} = [{Co(OH2)4}P4W24O92(POC6H5)2]14−; {P6W39V8} = [Rb3 ⊂ {VVVIV3O7(H2O)6}2{H6P6W39O147(H2O)3}]15−; {P2W12Mn4}6 = [{P2W12O48Mn4(acetylacetonate)2(acetate)}6]42−; {P8W48Mn16} = [{γ-P2W12O48Mn4(H2O)6}4(H2O)4]24−; and {P8W48} = [P8W48O184]40−.

Despite extensive exploration of transition-metal-containing P2W12 clusters, the crystal structure of {P2W12} (without coordination with other transition metals) and its structural transformation in aqueous solution are not well understood. Contant and Tézé reported that {P2W12} anions transform into several types of dimers and oligomers[21] that are yet to be discovered. Therefore, the chemistry of pure {P2W12} is complex and requires further investigation. Herein, we report crystal structure of {P2W12} and its structural transformation into two types of {WO(OH2)}4+-bridged oligomers: a Pacman-shaped [{WO(OH2)}2(HP2W12O48)2]22− ({P4W25}) dimer and a cyclic [{WO(OH2)}3(P2W12O48)3]30− ({P6W39}) trimer. The three anions were selectively isolated through the recrystallization of (NH4)12[α-H2P2W12O48] using an appropriate combination of counter cations, as illustrated in Scheme 2. The phase purity was confirmed through powder X-ray diffraction. 31P and 183W NMR analyses indicated that these anions decomposed in aqueous solutions.
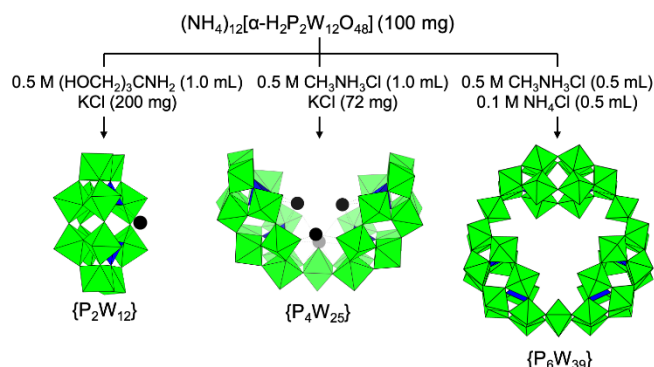
Scheme 2. Synthetic approaches and results of this study. Color scheme: blue, P; black, K; and green, W.

Results and Discussion

Crystal structure

Careful control of the crystallization conditions was necessary to produce the three phosphotungstates crystals. Single crystals of {P2W12} were prepared through recrystallization of (NH4)12[α-H2P2W12O48] from 0.5 M (HOCH2)3CNH2 solution (pH of the mixture was in the range of 9.3–9.4) in the presence of excess KCl. This recrystallization condition is similar to the formation condition of {P2W12}, which is significantly more basic than the crystallization condition of the [P8W48O184]40− tetramer.[21] {P2W12} crystallizes as K10.4(NH4)1.6[α-H2P2W12O48]·24H2O (**1**) in the orthorhombic space group *Pnma* and has a boat-shaped structure (Figure 1a) derived from [α-P2W18O62]6− by removing six tungsten atoms: one from each {W3} cap and four from the {W12} belt group (see Figure S1b). The four oxygen atoms of the phosphate groups are coordinating tungsten centers, confirming that {P2W12} is indeed an alpha isomer (in contrast to the gamma {P2W12} isomer found in copper-incorporated [P8W48O184]40− anions[23], hexameric [{γ-P2W12O48Mn4(acetylacetonate)2(acetate)}6]42− and tetrameric [{γ-P2W12O48Mn4(H2O)6}4(H2O)4]24− anions[22]—whose phosphate groups have one terminal oxygen atom, Figure S2). X-ray diffraction and elemental analyses revealed the presence of approximately 10.4 potassium cations surrounding the surface of {P2W12}; one of the potassium cations sits exactly on the center of the lacunary site via coordination with the oxygen atoms of phosphate (the mean K···OP distance is 2.83 Å). A space-filling model (Figure 1b) illustrates the size of potassium cation is just fit to cap the lacunary site similar to potassium salt of [P8W48O184]40−.[21, 24] Bond valence sum (BVS) calculations confirmed that all tungsten atoms were in the +6 oxidation state; complete lists of the BVS calculation results are summarized in Table S1. According to Contant and Tézé, the two protons of {P2W12} are non-dissociable and are located on two {W2} polar caps.[21] BVS values of oxygen atoms in the current {P2W12} model, unfortunately, do not indicate the protonation sites.
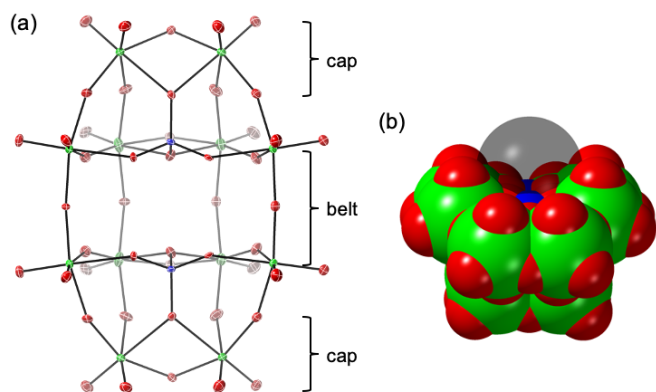
Figure 1. (a) Thermal ellipsoid plot (at the 50% probability level) of {P2W12} viewed from the lacunary site and (b) a space-filling model showing a potassium cation (translucent black sphere) that fits into the center of the lacunary site. Color scheme: green, W; blue, P; and red, O.

Dissolution of $(NH_4)_{12}[\alpha-H_2P_2W_{12}O_{48}]$ in 0.5 M CH_3NH_3Cl followed by the addition of KCl (pH of the mixture was in the range of 8.0–8.2) produced {P4W25} that crystallized as $K_{17}(NH_4)_5[\{WO(OH_2)\}(\alpha-HP_2W_{12}O_{48})_2]\cdot38H_2O$ (**2**) in the monoclinic system space group $P2/c$. As shown in Figure 2a, {P4W25} comprises two $\{\alpha-P_2W_{12}O_{48}\}^{14-}$ units connected with C_{2v} symmetry at their {W2} caps by a tungsten-oxo-aquo $\{WO(OH_2)\}^{4+}$ cation, resulting in a Pacman-like structure. As such, {P2W25} differs from $[H_2P_4W_{24}O_{94}]^{22-}$ whose structure is expected to contain corner-sharing of two $\{\alpha-P_2W_{12}O_{48}\}^{14-}$ without the linking $\{WO(OH_2)\}^{4+}$ unit.[21] Each $\{\alpha-P_2W_{12}O_{48}\}^{14-}$ of {P2W25} was monoprotonated, and BVS calculations revealed that the protonation site was not at the terminal oxygen atoms and {W2} cap oxygens, but at one of the bridging oxygen atoms, O32 (BVS = 1.25); protonation of one of the bridging oxygen atoms has been observed in $[\gamma-SiW_{10}O_{36}]^{8-}$.[25] The W–O bond distances of $\{WO(OH_2)\}^{4+}$ clearly indicate that O1 (d W1–O1 = 1.75 Å; BVS O1 = 1.57) is O^{2-}, whereas O50 (d W1–O50 = 2.38 Å; BVS O50 = 0.29) is an aquo ligand. The potassium counter cations can be categorized into three types: (i) K1 that caps the center of the lacunary site of $\{\alpha-P_2W_{12}O_{48}\}^{14-}$ units, (ii) K2 that caps the horseshoe-shaped semicircle formed by the two $\{\alpha-P_2W_{12}O_{48}\}^{14-}$ and $\{WO(OH_2)\}^{4+}$ units, and (iii) exterior K^+ that links {P4W25} to one another in the crystal packing (Figure S3). These K^+ ions may facilitate the formation of {P4W25} by preventing the addition of $\{\alpha-P_2W_{12}O_{48}\}^{14-}$ and $\{WO(OH_2)\}^{4+}$ units to the {P4W25} framework.

Finally, recrystallization of $(NH_4)_{12}[\alpha-H_2P_2W_{12}O_{48}]$ from a 1:1 v/v mixture of 0.5 M CH_3NH_3Cl and 0.1 M NH_4Cl in the absence of K^+ cations (pH of the mixture was 7.4–7.8) afforded {P6W39} as $(NH_4)_{15}(CH_3NH_3)_{15}[\{WO(OH_2)\}_3(\alpha-P_2W_{12}O_{48})_3]\cdot98H_2O$ (**3**). Compound **3** crystallized in the trigonal space group $P6_3/mmc$ with one-sixth of the molecule in the asymmetric unit. The {P6W39} anion had a cyclic structure composed of three $\{\alpha-P_2W_{12}O_{48}\}^{14-}$ units connected by three $\{WO(OH_2)\}^{4+}$ cations (Figure 2b). The overall molecule exhibits D_{3h} symmetry. The W–O bond distances (W1–O1, 1.71, and W1–O17, 2.26 Å) and BVS values (O1, 1.75, and O17, 0.40) confirmed that O1 and O17 were oxo and aquo ligands on the exterior and interior surfaces of the cluster, respectively. {P6W39} contained a cavity (Figure S4a) with an estimated volume of 243.83 Å³. In addition, the crystal packing of **3** contained cavities (Figure S4b). These cavities are most likely occupied by counter-cations (methylammonium and ammonium) and water solvates whose location could not be determined through X-ray diffraction. Cronin et al. reported an ammonium salt

of $[P_8W_{48}O_{184}]^{40-}$ in which ammonium cations interact with inner oxygen atoms.[24]

To the best of our knowledge, the isolation of the {P6W39} anion without coordination to transition metal cations is unprecedented. The {P6W39} framework was first reported by Wang et al. as a coordination complex of manganese(II), nickel(II), or copper(II) cations, which were coordinated to the aperture of the cavity of the cluster.[19c] Years later, the same group reported lanthanide- and cobalt-coordinated {P6W39},[19a, 19b] whereas Kortz et al. reported that {P6W39} with mixed-valence vanadium(IV/V) clusters capped the cavity of the cluster.[19d] This is in contrast with the selenium analog $[Se_6W_{39}O_{141}(OH_2)_3]^{24-}$ that is isolable without the stabilizing transition metal cations.[26]
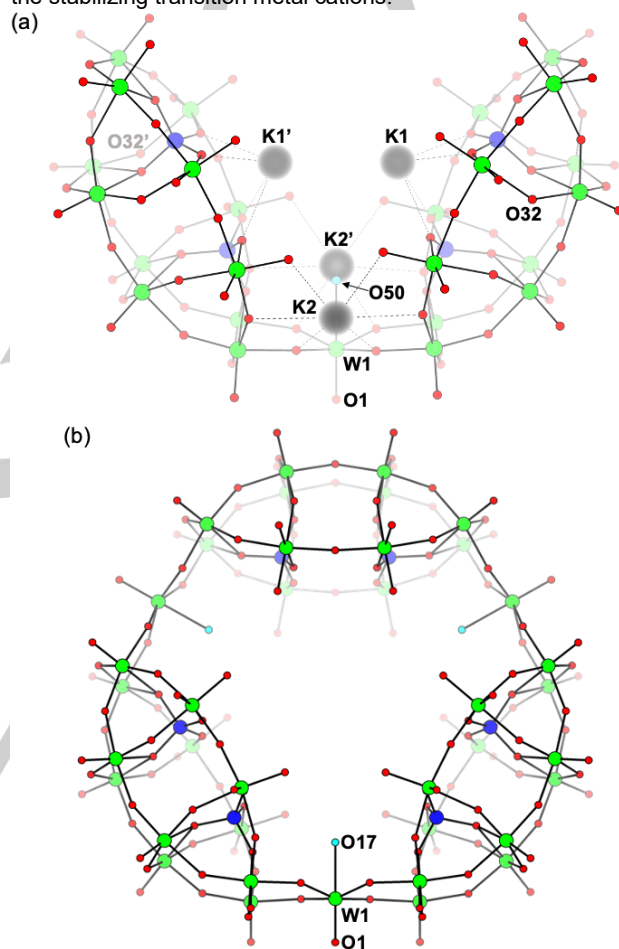
Figure 2. Ball-and-stick models of (a) {P4W25} with four potassium cations (black translucent circles) displayed and (b) {P6W39}. Color scheme: green, W; blue, P; red, O; and cyan, aquo ligands. The prime (') symbols indicate atoms related to the respective atom by two-fold rotation.

Solid-state bulk characterizations

The powder X-ray diffraction patterns of **1**–**3** (Figure 3) were in agreement with the theoretical patterns simulated using a single-crystal structure, confirming the phase purity of the bulk solids. The powder pattern of **3** was collected at −150 °C because at room temperature, most of the diffraction maxima could not be observed (Figure S5) owing to evaporation of crystallization water, re-orientation of methylammonium counter-cations,[27] or both. Because the low-temperature powder pattern was collected using a single-crystal diffractometer, the peaks were significantly broadened, hindering the observation of closely separated peaks (for instance, the second diffraction maximum at 2θ = 2.6° is a

composite of two peaks that theoretically appear at 2θ = 2.48 and 2.74°). The obtained pattern behaves like an envelope and is informative enough to support a phase purity of **3**. Compounds **1**–**3** exhibited similar Fourier transform infrared (FTIR, Figure S6) spectra in the P–O and W–O vibration regions because they were built from the same $\{P_2W_{12}\}$ building blocks.
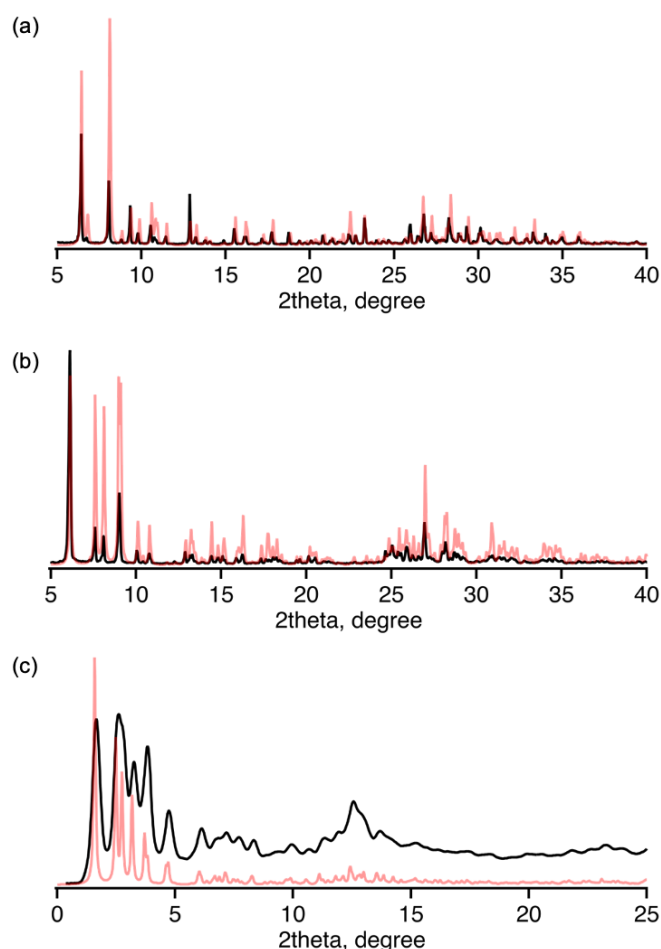
Figure 3. Powder X-ray diffraction patterns of (a) **1**, (b) **2**, and (**3**); opaque black traces and translucent red traces are observed and simulated patterns, respectively.

Solution-state structure

To investigate the structural integrity of **1**–**3** upon dissolution, we analyzed their dilute aqueous solution (approximately 10 mg sample in 0.6 mL deuterium oxide) using ^{31}P NMR spectroscopy. If the $\{P_2W_{12}\}$, $\{P_4W_{25}\}$, and $\{P_6W_{39}\}$ anions dissolve intact in the solution, their ^{31}P NMR spectra must exhibit one, two, and one signals, respectively, as required by their solid-state symmetry. Figure 4a shows the ^{31}P NMR spectra of freshly prepared solutions of **1**–**3** in comparison to the ^{31}P NMR spectrum of a freshly prepared solution of $(NH_4)_{12}[\alpha-H_2P_2W_{12}O_{48}]$. Both **1** and $(NH_4)_{12}[\alpha-H_2P_2W_{12}O_{48}]$ contain $\{P_2W_{12}\}$ anions and show a single ^{31}P signal at −9.11 and −9.64 ppm, respectively; the ^{31}P signal of $(NH_4)_{12}[\alpha-H_2P_2W_{12}O_{48}]$ is shifted upfield owing to interactions of the phosphato groups with ammonium cations. Cronin et al. also reported a similar chemical shift difference between potassium- and ammonium containing $[P_8W_{48}O_{184}]^{40-}$ anions.[24] The ^{31}P NMR spectrum of **2** shows only one peak at −9.16 ppm, indicating the immediate decomposition of $\{P_4W_{25}\}$ into $\{P_2W_{12}\}$ on dissolution. A fresh solution of **3** exhibited a sharp signal at −9.69 ppm (full

width at half maximum FWHM = 4 Hz, compared to **1** with FWHM = 31 Hz). On prolonged standing, at least three new peaks at δ = −8.78, −9.56, and −10.9 ppm were detected (Figure 4b, trace ii–iv), and their intensity increased as the solution aged. The broad peak at −9.56 ppm is tentatively assigned to the monomeric $\{P_2W_{12}\}$ anions produced by the hydrolysis of $\{P_6W_{39}\}$. This assumption is supported by the ^{31}P NMR spectrum of a fresh mixture of **3** and $(NH_4)_{12}[\alpha-H_2P_2W_{12}O_{48}]$ (Figure 4b, trace v) that exhibits a sharp peak at −9.72 and a broad peak at −9.61 ppm, a trend similar to the spectra of aged solution of **3**. Time-dependent ^{31}P NMR spectra of **1** and **2** are shown in Figure S7. ^{31}P NMR spectroscopy indicated that the $\{P_4W_{25}\}$ and $\{P_6W_{39}\}$ anions were hydrolyzed upon dissolution in aqueous media, generating metastable $\{P_2W_{12}\}$ anions that underwent further decomposition reactions. Consequently, our efforts to collect ^{183}W NMR spectra of concentrated solutions of **1**–**3** (500 mg in 3.0 mL of 1 M LiCl-D_2O) failed to produce reliable spectra for unambiguous interpretations (Figure S8), while Baker et al. [8] and Contant and Tézé[21] reported difficulties in obtaining informative ^{183}W NMR spectra of $\{P_2W_{12}\}$ anions under several conditions (such as the use of Na or Li salt or varying the solution pH from 4.5 to 8).
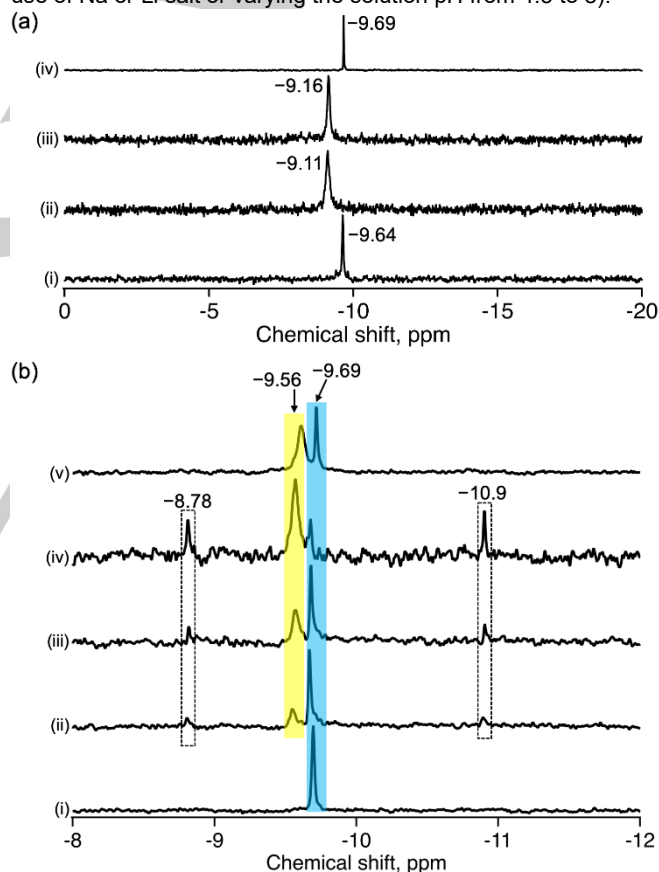
Figure 4. ^{31}P NMR spectra of (a) $(NH_4)_{12}[\alpha-H_2P_2W_{12}O_{48}]$ (trace i), **1** (trace ii), **2** (trace iii), and **3** (trace iv) and (b) **3** at 0 h (trace i), 2 h (trace ii), 4 h (trace iii), 10 h (trace iv), and a mixture of **3** (ca. 10 mg) and $(NH_4)_{12}[\alpha-H_2P_2W_{12}O_{48}]$ (ca. 10 mg) at 0 h (trace v). All solids were dissolved in deuterium oxide. The numbers indicate the chemical shift of the signals.

Conclusion

We determined the X-ray crystal structure of the metastable hexalacunary Wells-Dawson $\{P_2W_{12}\}$ and confirmed that the anion is indeed an alpha isomer derived by removing six tungsten atoms from $[\alpha-P_2W_{18}O_{62}]^{6-}$ for the first time after the discovery of $\{P_2W_{12}\}$ by Contant and Ciabrini in 1977. In addition, we observed

that the anion oligomerizes in near-neutral solution into a $\{WO(OH_2)\}^{4+}$-bridged pacman-shaped dimer $\{P_4W_{25}\}$ and a cyclic trimer $\{P_6W_{39}\}$. These anions were selectively crystallized using an appropriate combination of countercations without stabilization by coordination with transition metal cations. This study further emphasizes the potential of countercations as structure-directing agents for the synthesis and crystallization of metastable polyoxometalate clusters.

Experimental Section

Materials and analytical methods. $(NH_4)_{12}[α-H_2P_2W_{12}O_{48}]\cdot 10H_2O$ was prepared following the procedure reported in a previous study.[24] However, the starting $(NH_4)_6[α-P_2W_{18}O_{62}]$ was synthesized according to Nadjo's method[28] (using NH_4Cl instead of KCl to precipitate Dawson anions), and the obtained $(NH_4)_{12}[α-H_2P_2W_{12}O_{48}]$ was rinsed several times with ethanol and ether. In addition, we monitored pH changes during the formation of $(NH_4)_{12}[-H_2P_2W_{12}O_{48}]$ and observed that the pH of the $(NH_4)_6[α-P_2W_{18}O_{62}]/$ $(HOCH_2)_3CNH_2$ mixture was approximately 8.3, which decreased to 8.16 when NH_4Cl was added. After the addition of an aqueous $(NH_4)_2CO_3$ solution, the pH of the mixture was 8.5, which increased to 8.62 (within 3 min) at which point solids of $(NH_4)_{12}[α-H_2P_2W_{12}O_{48}]$ began to form. After vigorous stirring for 15 min, more solids of $(NH_4)_{12}[α-H_2P_2W_{12}O_{48}]$ were formed and the pH of the mixture was 8.69. Freshly prepared $(NH_4)_{12}[α-H_2P_2W_{12}O_{48}]$ was used to synthesize **1–3** to ensure purity, yield, and reproducibility. All the other chemicals were purchased and used as received. Homemade water (Elix Essential) was also used. FT-IR spectra were collected using a KBr disc on a Thermo Scientific Nicolet 6700 FT-IR spectrometer. Powder X-ray diffraction patterns of **1** and **2** were recorded on a Bruker D2 Phaser (Cu Kα radiation, λ = 1.54184 Å) equipped with 1D Lynxeye detector at ambient temperature, whereas powder pattern of **3** was collected on a Bruker SMART APEX2 CCD single-crystal diffractometer (Mo Kα radiation, λ = 0.71073 Å) at −150 °C as follows: a small amount of crystals was suspended in mineral oil and was slightly ground using a plastic spatula and the resulting microcrystalline paste was loaded onto a 0.1 mm nylon loop and mounted on the goniometer head. Diffraction rings were collected using a standard 360° phi rotation technique with an exposure time of 60 s; the detector was positioned at 2θ = 0° and its distance to the sample was set at 60 mm (Figure S9). ^{31}P NMR spectra were recorded using an Agilent Variant System 500 (500 MHz; P resonance frequency = 202.378 MHz), and the chemical shifts were referenced to an external H_3PO_4 standard (δ = 0 ppm). ^{183}W NMR spectra were collected on a JEOL ECA500 spectrometer (500 MHz, W resonance frequency = 20.839 MHz); the chemical shifts were referenced to an external 2 M Na_2WO_4 (δ = 0 ppm) in deuterium oxide. Thermogravimetric (TG) analyses were conducted on a Hitachi SII TG/DTA analyzer under a constant flow of air (100 mL/minute) and a heating rate of 10 °C/minute; thermograms are shown in Figure S10. Elemental analyses were performed by Mikroanalytisches Labor Pascher (Remagen, Germany).

Synthesis of $K_{10.4}(NH_4)_{1.6}[α-H_2P_2W_{12}O_{48}]\cdot 24H_2O$ (1). In a water bath set at 35 °C, freshly prepared $(NH_4)_{12}[α-H_2P_2W_{12}O_{48}]\cdot 10H_2O$ (100 mg; 0.03 mmol) was dissolved (within 5 seconds) in 0.5 M $(HOCH_2)_3CNH_2$ (1.0 mL) to yield a limpid solution into which granule KCl (200 mg; 2.68 mmol) was immediately added. The reaction vessel was manually shaken to dissolve most KCl (within 10 s; prolonged warming should be avoided to maintain high yields) and was left at 27 °C to deposit block crystals. The crystals were harvested after standing for 2 h and were subsequently air-dried. The pH of the reaction mixture before and after crystallization was 9.29 and 9.42, respectively. Yield = 82.6 mg (73% based on W). Elem. Anal. calcd for **1**·$0.2(HOCH_2)_3CNH_3Cl$: C, 0.24; H, 1.51; Cl, 0.18; K, 10.33; N, 0.64; P, 1.57; W, 56.02. Found: C, 0.52; H, 1.26; Cl, 0.29; K, 10.1; N, 0.34; P, 1.54; W, 56. FT-IR (KBr, cm$^{−1}$): 1132 (m, sh), 1084 (m, sh), 1013 (w, sh), 971–962 (br), 910 (s, sh), 870 (s, br), 825 (s, br), 750 (s, br), and 685 (s, br). TG analyses established a total weight loss of 11.19% at 560 °C,

corresponding to the decomposition of one mole of **1** to $P_2O_5\cdot 12WO_3\cdot 5.2K_2O$, $1.6NH_3$, and $25.8H_2O$ (calcd 11.07%).

Synthesis of $K_{17}(NH_4)_5[\{WO(OH_2)\}(α-HP_2W_{12}O_{48})_2]\cdot 38H_2O$ (2). In a water bath set at 35 °C, freshly prepared $(NH_4)_{12}[α-H_2P_2W_{12}O_{48}]\cdot 10H_2O$ (100 mg; 0.03 mmol) was dissolved (within 5 seconds) in 0.5 M CH_3NH_3Cl (1.0 mL) to yield a limpid solution into which granule KCl (72.0 mg; 0.97 mmol) was immediately added. The reaction vessel was manually shaken to dissolve most of the KCl (within 10 s), during which crystals of **2** started to form. The mixture was removed from the water bath and was left at 27 °C to deposit more crystals. The crystals were harvested after standing for an hour and were subsequently air-dried. The pH of the reaction mixture before and after crystallization was 7.99 and 8.20, respectively. Yield = 37.2 mg (34% based on W). Elem. Anal. calcd for **2**·$3CH_3NH_3Cl$: C, 0.45; H, 1.50; Cl, 1.34; K, 8.38; N, 1.41; P, 1.56; W, 57.92. Found: C, 0.4; H, 1.26; Cl, 1.4; K, 8.39; N, 1.07; P, 1.53; W, 57.9. FT-IR (KBr, cm$^{−1}$): 1456–1402 (w, br), 1138 (m, sh), 1084 (m, sh), 1014 (w, sh), 979 (w), 916 (s, sh), 866–783 (s, br), and 707 (s, br). TG analyses established a total weight loss of 10.84% at 630 °C, corresponding to the decomposition of one mole of **2** to $2P_2O_5\cdot 25WO_3\cdot 8.5K_2O$, $5NH_3$, and $42.5H_2O$ (calcd 11.01%).

Synthesis of $(NH_4)_{15}(CH_3NH_3)_{15}[\{WO(OH_2)\}_3(α-P_2W_{12}O_{48})_3]\cdot 98H_2O$ (3). In a water bath set at 35 °C, freshly prepared $(NH_4)_{12}[α-H_2P_2W_{12}O_{48}]\cdot 10H_2O$ (200 mg; 0.06 mmol) was dissolved (within 5 seconds) in 0.5 M CH_3NH_3Cl (1.0 mL) to afford a limpid solution into which 0.1 M NH_4Cl (1.0 mL) was added. The clear solution was allowed to evaporate in a loosely covered glass vial at 27 °C. Crystals of **3** began to appear after standing overnight and were harvested after 48 h. The pH of the reaction mixture before and after crystallization was 7.80 and 7.39, respectively. Yield = 55.2 mg (25% based on W). Elem. Anal. calcd for **3**·$0.2CH_3NH_3Cl$: C, 1.49; H, 2.90; Cl, 0.06; N, 3.44; P, 1.51; W, 58.32. Found: C, 1.44; H, 2.69; Cl, 0.07; N, 3.59; P, 1.49; W, 58.3. FT-IR (KBr, cm$^{−1}$): 1500–1400 (br), 1136 (m, sh), 1086 (m, sh), 1018 (w, sh), 986 (w, sh), 918 (s, sh), 862–781 (s, br), 714 (s, br), and 614 (s, br). TG analyses established a total weight loss of 22.91% at 540 °C, corresponding to the decomposition of one mole of **3** to $3P_2O_5\cdot 39WO_3$, $15NH_3$, $15CH_3NH_2$, and $116H_2O$ (calcd 22.90%).

X-ray crystallography. Single crystals suitable for X-ray analysis were suspended in mineral oil and mounted on a goniometer head under a nitrogen stream. Intensity data were collected at −150°C on a Bruker SMART APEX II diffractometer equipped with a CCD detector and a Mo Kα radiation (λ = 0.71073 Å) source monochromated by layered confocal mirrors. Indexing, unit cell determination, and data reduction were performed using a Bruker APEX3 suite.[29] Multi-scan absorption corrections were applied using the SADABS software.[29] The initial structure was solved using *SHELXT*[30] and refined using *SHELXL*[31] running on a *ShelXle* interface.[32] All non-hydrogen atoms were refined anisotropically. No ammonium cations or water solvates were identified. Methylammonium cations could not be located because of disorder. Detailed crystallographic parameters are listed in Table 1. Deposition number(s) 2235503 (for **1**), 2235504 (for **2**), 2235505 (for **3**) contain(s) the supplementary crystallographic data for this paper. These data are provided free of charge by the joint Cambridge Crystallographic Data Centre and Fachinformationszentrum Karlsruhe Access Structures service.

BVS calculation. The BVS values were determined as expressed in Equation 1, which relates the bond length r_{ij} between two atoms i and j in the observed crystal with valence of the atom $V_{,i}$. The constant B, equal to 0.37 Å, was used in the calculation, along with the bond valence parameter for a specific atom pair. In this case, the values r'_0 = 1.917 for W^{VI}–O and 1.617 Å for P^V–O pairs[33] were used to determine the BVS of tungsten and oxygen atoms in **1–3**.

WILEY-VCH

$$V_i = \sum_j \exp\left(\frac{{r'}_0 - r_{ij}}{B}\right) \quad\quad (1)$$

Acknowledgements

Table 1. Crystallographic parameters for **1**–**3**. *Formula and formula weight based solely on crystallographic analysis. $R_1 = \{\Sigma||F_o|-|F_c||\}/\{\Sigma|F_o|\}$ and $wR_2 = [\Sigma w(F_o{}^2-F_c{}^2)/\Sigma wF_o{}^2]^{1/2}$.

Compound	1	2	3
Formula unit*	$K_{10.4}O_{66.8}P_2W_{12}$	$K_{15.4}O_{133}P_4W_{25}$	$C_{4.05}H_{24.28}N_{8.44}O_{188.26}P_6W_{39}$
Formula weight* (g/mol)	3743.58	7450.27	10559.49
Crystal system	Orthorhombic	Monoclinic	Hexagonal
Space group (number)	*Pnma* (62)	*P2/c* (13)	*P6₃/mmc* (194)
a, Å	17.8907(9)	20.3192(9)	29.6867(10)
b, Å	19.9932(10)	14.4014(7)	29.6867(10)
c, Å	18.8267(10)	22.8392(10)	21.3039(10)
α, °	90	90	90
β, °	90	104.601(1)	90
γ, °	90	90	120
V, Å³	6734.2(6)	6467.5(5)	16259.7(13)
Z	4	2	2
D_{calc} (g/cm³)	3.692	3.826	2.157
μ (mm⁻¹)	21.212	22.795	13.828
Radiation	Mo Kα (λ = 0.71073 Å)	Mo Kα (λ = 0.71073 Å)	Mo Kα (λ = 0.71073 Å)
Temperature (K)	123(2)	123(2)	123(2)
F_{000}	6600	6533	9179
Θ range	1.486 to 27.895°	1.414 to 27.520°	1.241 to 25.378°
Index ranges	−23 ≤ h ≤ 23; −26 ≤ k ≤ 26; −24 ≤ l ≤ 24	−13 ≤ h ≤ 26; −18 ≤ k ≤ 18; −29 ≤ l ≤ 29	−35 ≤ h ≤ 35; −35 ≤ k ≤ 33; −25 ≤ l ≤ 17
No. of reflections collected	58067	36903	79646
Unique reflections (R_{int})	8254 (0.0422)	14817 (0.0393)	5445 (0.0622)
Data/restrains/parameters	8254/0/448	14817/48/882	5445/67/233
R indexes [I>2σ(I)]	$R_1 = 0.0270; wR_2 = 0.0663$	$R_1 = 0.0348; wR_2 = 0.0732$	$R_1 = 0.0327; wR_2 = 0.0770$
R indexes (all data)	$R_1 = 0.0331; wR_2 = 0.0692$	$R_1 = 0.0492; wR_2 = 0.0784$	$R_1 = 0.0491; wR_2 = 0.0882$
G.O.F	1.034	1.030	1.073
$(\Delta/\sigma)_{max}$	0.001	0.002	0.001
$\Delta\rho_{max/min}$ (e A⁻³)	2.148/−1.703	2.679/−1.534	1.620/−1.658
CCDC number	2235503	2235504	2235505

Keywords: lacunary Dawson • phosphotungstate • polyoxometalate • X-ray crystallography

[1] S. S. Wang, G. Y. Yang, *Chem. Rev.* **2015**, *115*, 4893-4962.

[2] N. Ogiwara, T. Iwano, T. Ito, S. Uchida, *Coord. Chem. Rev.* **2022**, *462*, 214524.

[3] J. M. Clemente-Juan, E. Coronado, A. Gaita-Arino, *Chem. Soc. Rev.* **2012**, *41*, 7464-7478.

[4] a) K. Sahiro, Y. Kawato, K. Koike, T. Sano, T. Nakai, M. Sadakane, *Sci. Rep.* **2022**, *12*, 7554; b) A. Bijelic, A. Rompel, *Coord. Chem. Rev.* **2015**, *299*, 22-38.

[5] a) S. T. Zheng, G. Y. Yang, *Chem. Soc. Rev.* **2012**, *41*, 7623-7646; b) Z.-J. Liu, X.-L. Wang, C. Qin, Z.-M. Zhang, Y.-G. Li, W.-L. Chen, E.-B. Wang, *Coord. Chem. Rev.* **2016**, *313*, 94-110.

[6] R. Contant, W. G. Klemperer, O. Yaghi, in *Inorg. Synth., Vol. 27*, **1990**, pp. 104-111.

[7] R. Contant, J.-P. Ciabrini, *J. Chem. Res., Synop .* **1977**, 222.

[8] R. Acerete, C. F. Hammer, L. C. W. Baker, *Inorg. Chem.* **1984**, *23*, 1478-1482.

[9] W. J. Xuan, C. Botuha, B. Hasenknopf, S. Thorimbert, *Chem. Eur. J.* **2015**, *21*, 16512-16516.

[10] D. A. Judd, Q. Chen, C. F. Campana, C. L. Hill, *J. Am. Chem. Soc.* **1997**, *119*, 5461-5462.

[11] R. Contant, M. Abbessi, R. Thouvenot, G. Herve, *Inorg. Chem.* **2004**, *43*, 3597-3604.

[12] B. Godin, Y. G. Chen, J. Vaissermann, L. Ruhlmann, M. Verdaguer, P. Gouzerh, *Angew. Chem. Int. Ed.* **2005**, *44*, 3072-3075.

[13] D. Zhang, F. Cao, P. Ma, C. Zhang, Y. Song, Z. Liang, X. Hu, J. Wang, J. Niu, *Chem. Eur. J.* **2015**, *21*, 17683-17690.

[14] D. Zhang, C. Zhang, P. Ma, B. S. Bassil, R. Al-Oweini, U. Kortz, J. Wang, J. Niu, *Inorg. Chem. Front.* **2015**, *2*, 254-262.

[15] X. Yi, N. V. Izarova, P. Kogerler, *Chem. Commun.* **2018**, *54*, 2216-2219.

[16] T. Iftikhar, N. V. Izarova, J. van Leusen, P. Kogerler, *Chem. Eur. J.* **2021**, *27*, 13376-13383.

[17]   F. Hussain, U. Kortz, B. Keita, L. Nadjo, M. T. Pope, *Inorg. Chem.* **2006**, *45*, 761-766.

[18]   Z. Zhang, S. Yao, Y. Qi, Y. Li, Y. Wang, E. Wang, *Dalton Trans* **2008**, 3051-3053.

[19]   a) S. Yao, Z. Zhang, Y. Li, E. Wang, *Dalton Trans.* **2010**, *39*, 3884-3889; b) S. Yao, Z. Zhang, Y. Li, Y. Lu, E. Wang, Z. Su, *Cryst. Growth Des.* **2010**, *10*, 135-139; c) Z.-M. Zhang, S. Yao, Y.-G. Li, Y.-H. Wang, Y.-F. Qi, E.-B. Wang, *Chem. Commun.* **2008**, 1650-1652; d) A. S. Assran, N. V. Izarova, U. Kortz, *CrystEngComm* **2010**, *12*, 2684-2686.

[20]   S. S. Mal, M. H. Dickman, U. Kortz, *Chem. Eur. J.* **2008**, *14*, 9851-9855.

[21]   R. Contant, A. Teze, *Inorg. Chem.* **1985**, *24*, 4610-4614.

[22]   T. Minato, K. Suzuki, K. Yamaguchi, N. Mizuno, *Angew. Chem. Int. Ed.* **2016**, *55*, 9630-9633.

[23]   a) X. Yi, N. V. Izarova, T. Iftikhar, J. van Leusen, P. Kogerler, *Inorg. Chem.* **2019**, *58*, 9378-9386; b) Y. Koizumi, K. Yonesato, K. Yamaguchi, K. Suzuki, *Inorg. Chem.* **2022**, *61*, 9841-9848; c) S. Sasaki, K. Yonesato, N. Mizuno, K. Yamaguchi, K. Suzuki, *Inorg. Chem.* **2019**, *58*, 7722-7729.

[24]   T. Boyd, S. G. Mitchell, D. Gabb, D. L. Long, L. Cronin, *Chem. Eur. J.* **2011**, *17*, 12010-12014.

[25]   K. Sugahara, S. Kuzuya, T. Hirano, K. Kamata, N. Mizuno, *Inorg. Chem.* **2012**, *51*, 7932-7939.

[26]   J. M. Cameron, J. Gao, L. Vila-Nadal, D. L. Long, L. Cronin, *Chem. Commun.* **2014**, *50*, 2155-2157.

[27]   N. C. Sukmana, Sugiarto, J. Shinogi, A. Yamamoto, A. Higashiura, T. Sakaguchi, M. Sadakane, *Eur. J. Inorg. Chem.* **2022**, e202200322.

[28]   I.-M. Mbomekalle, Y. W. Lu, B. Keita, L. Nadjo, *Inorg. Chem. Commun.* **2004**, *7*, 86-90.

[29]   Bruker, *APEX3, SADABS, SAINT* **2016**.

[30]   G. M. Sheldrick, *Acta Crystallogr., Sect. A: Found. Adv.* **2015**, *71*, 3-8.

[31]   G. M. Sheldrick, *Acta Crystallogr., Sect. C: Struct. Chem.* **2015**, *71*, 3-8.

[32]   C. B. Hubschle, G. M. Sheldrick, B. Dittrich, *J. Appl. Crystallogr.* **2011**, *44*, 1281-1284.

[33]   N. E. Brese, M. O'Keeffe, *Acta Crystallogr. Sect. B: Struct. Sci.* **1991**, *47*, 192-197.

Entry for the Table of Contents
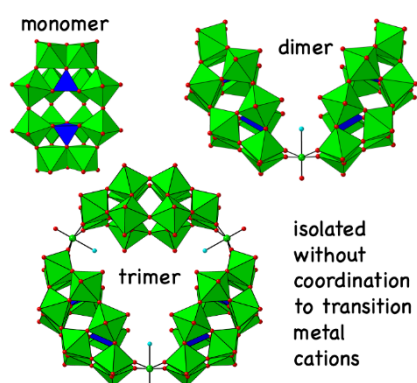
The first crystal structure of the metastable hexalacunary Wells-Dawson $[\alpha\text{-}H_2P_2W_{12}O_{48}]^{12-}$ ($\{P_2W_{12}\}$). By using a proper combination of counter cations, the anion selectively transforms into a $\{WO(OH_2)\}^{4+}$-bridged Pacman-shaped $[\{WO(OH_2)\}(\alpha\text{-}HP_2W_{12}O_{48})_2]^{22-}$ ($\{P4W25\}$) dimer or a cyclic $[\{WO(OH_2)\}_3(P_2W_{12}O_{48})_3]^{30-}$ ($\{P_6W_{39}\}$) trimer without coordination to transition metal cations.

Twitter: @Sadakane_Lab

Contents

Table S1. BVS calculation results for **1** and the labeling scheme.

	1
Tungsten	**_O_-bridging**
W1: 6.18	O2: 1.99
W2: 6.08	O4: 2.06
W3: 6.02	O6: 1.84
W4: 6.12	O8: 1.81
W5: 6.01	O10: 1.43
W6: 6.00	O11: 1.94
	O15: 1.92
Phosphate	O16: 1.59
P1: 4.96	O17: 1.66
O12: 1.91	O19: 2.12
O13: 1.87	O21: 1.98
O14: 1.92	
O24: 1.87	
_O_-terminal	
O1: 1.55	
O3: 1.56	
O5: 1.57	
O7: 1.60	
O9: 1.54	
O18: 1.63	
O20: 1.55	
O22: 1.55	
O23: 1.60	
O25: 1.52	
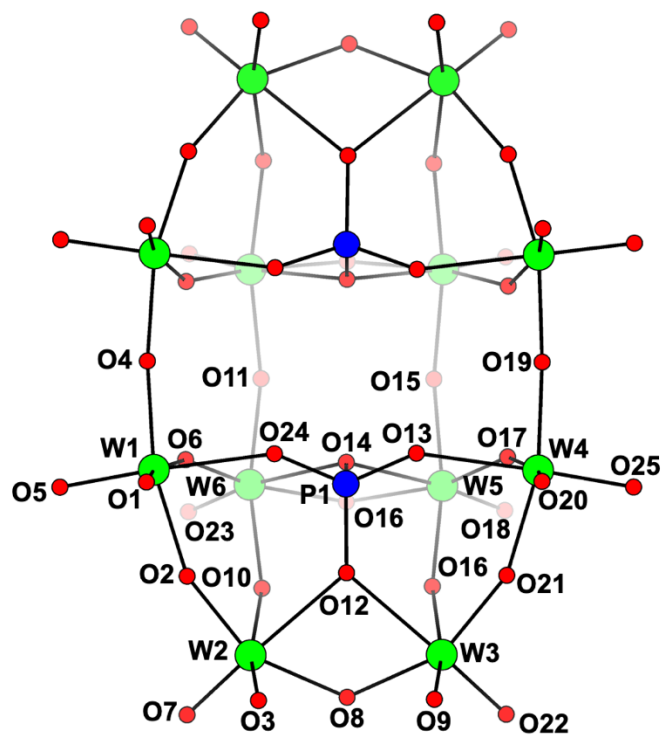
Table S2. BVS calculation results for **2** and the labeling scheme. Only half of the {P₄W₂₅} molecule (the asymmetric unit) is shown to improve visibility. O32 is the protonation site, and O50 is an aquo ligand.

2	
Tungsten	***O*-bridging**
W1: 6.11	O2: 1.93
W2: 6.06	O3: 1.88
W3: 6.02	O5: 1.80
W4: 6.09	O7: 1.90
W5: 6.13	O9: 1.88
W6: 6.15	O14: 1.86
W7: 6.16	O15: 1.90
W8: 5.99	O16: 2.10
W9: 6.14	O17: 2.11
W10: 6.25	O18: 1.91
W11:6.12	O20: 1.85
W12: 6.04	O21: 1.64
W13: 5.97	O22: 1.83
	O23: 1.57
Phosphate	O24: 2.06
P1: 4.99	O25: 2.03
O8: 1.90	**O32: 1.25**
O12: 1.86	O34: 1.86
O13: 1.81	O35: 1.63
O19: 1.98	O36: 1.87
P2: 4.96	O37: 1.58
O30: 1.81	O38: 1.88
O31: 1.86	O39: 1.88
O33: 1.93	O40: 2.01
O41: 1.94	O42: 2.02
	O44: 1.81
***O*-terminal**	
O1: 1.57	
O4: 1.66	
O6: 1.64	
O10: 1.55	
O11: 1.59	
O26: 1.64	
O27: 1.52	
O28: 1.52	
O29: 1.61	
O43: 1.56	
O45: 1.52	
O46: 1.58	
O47: 1.55	
O48: 1.62	
O49: 1.50	
O50: 0.29	

S3
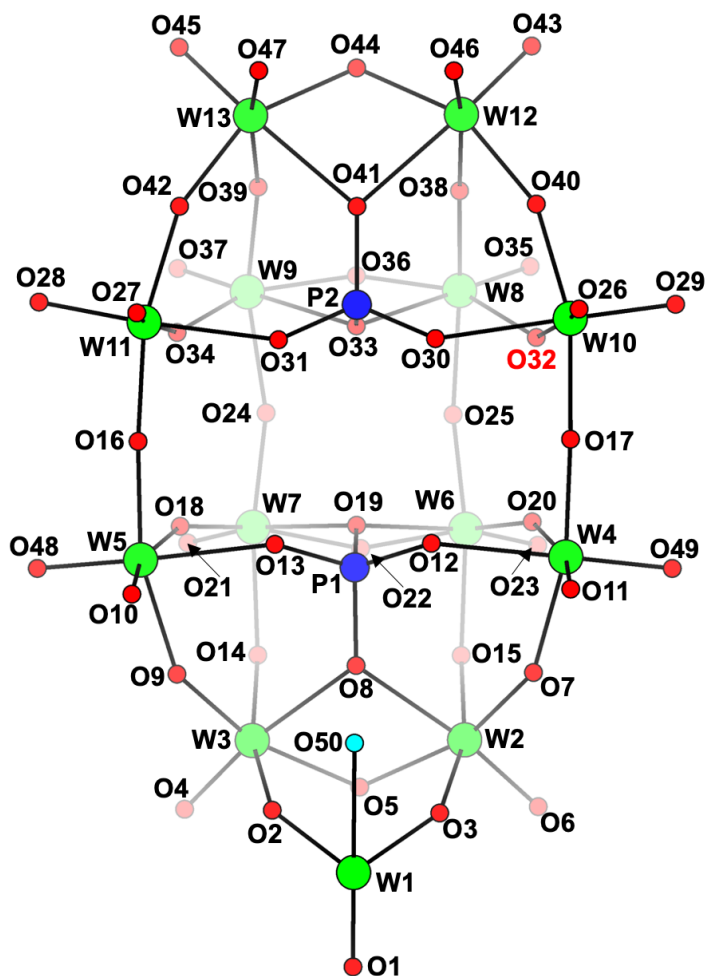
Table S3. BVS calculation results for **3** and the labeling scheme.

3
Tungsten
W1: 6.26
W2: 6.08
W3: 6.10
W4: 6.14
Phosphate
P1: 5.00
O5: 1.94
O11: 1.55
O12: 1.85
O-terminal
O1: 1.75
O4: 1.68
O8: 1.49
O10: 1.57
O15: 1.65
O17: 0.40
O-bridging
O2: 1.92
O3: 1.84
O6: 1.98
O7: 1.94
O9: 2.13
O13: 2.03
O14: 1.82
O16:1.93
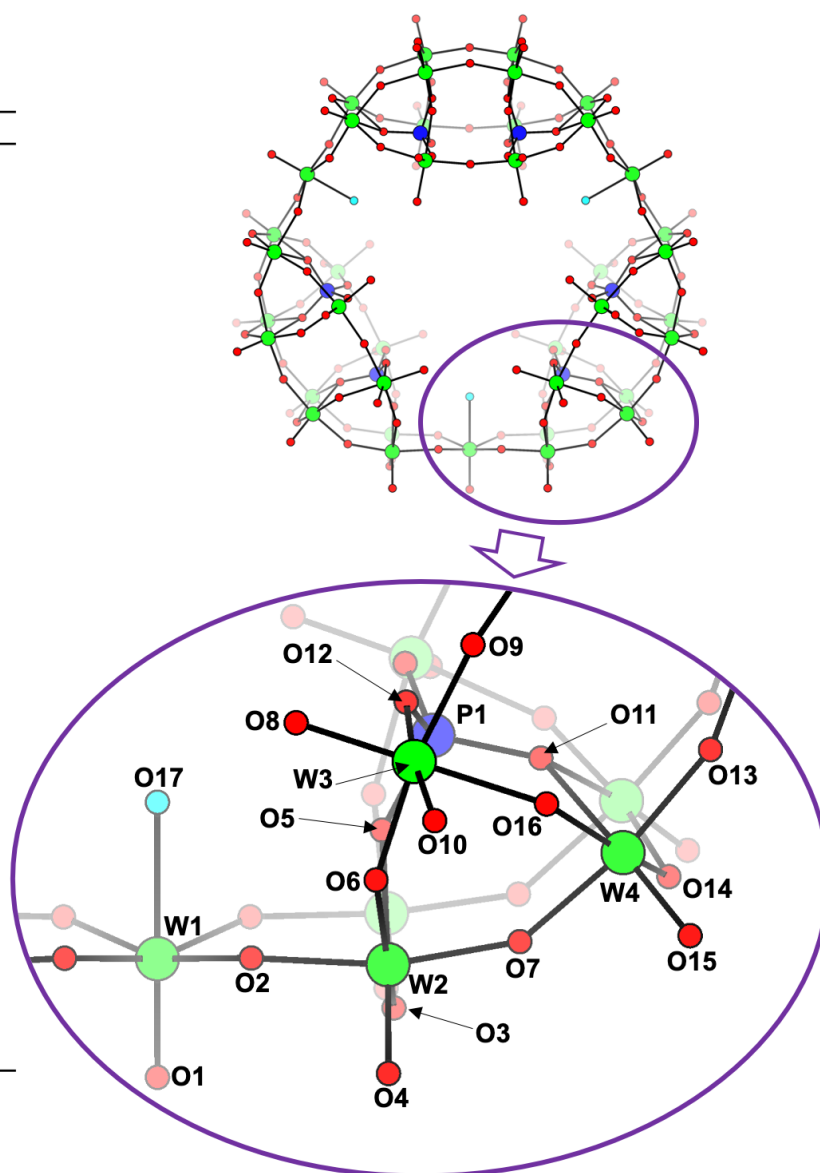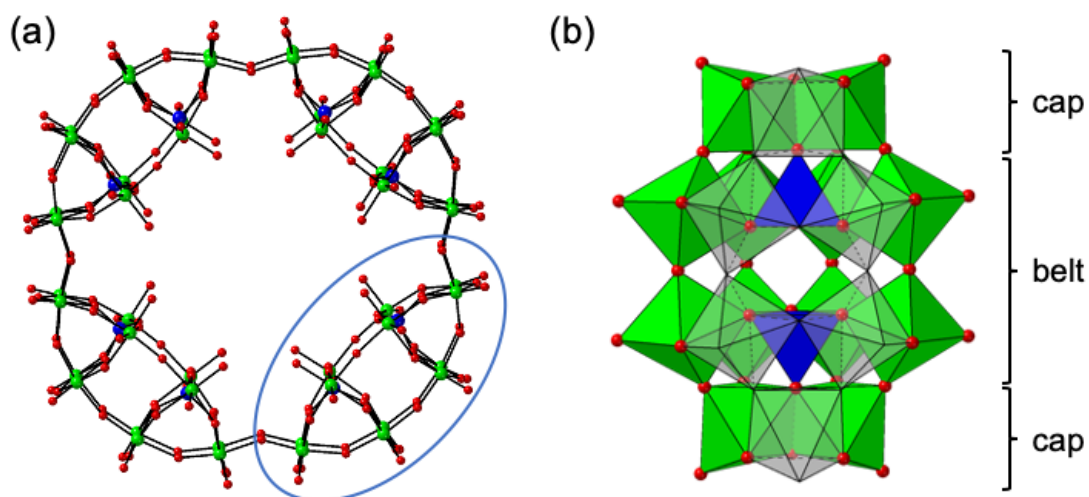
Figure S1. (a) Structure of $[P_8W_{48}O_{184}]^{40-}$ with one $[\alpha\text{-}P_2W_{12}O_{48}]^{14-}$ unit marked by a blue circle and (b) Currently accepted structure of $[\alpha\text{-}P_2W_{12}O_{48}]^{14-}$ derived by removing a $\{W_6O_{14}\}$ fragment (translucent polyhedra) from an $[\alpha\text{-}P_2W_{18}O_{62}]^{6-}$ anion. Color code: green, W; blue, P; red, O.
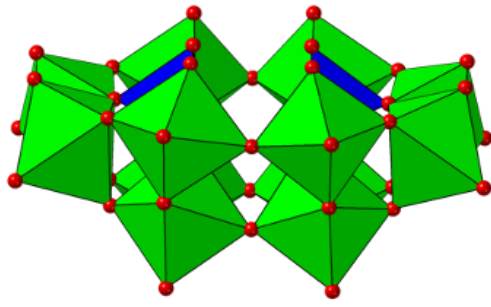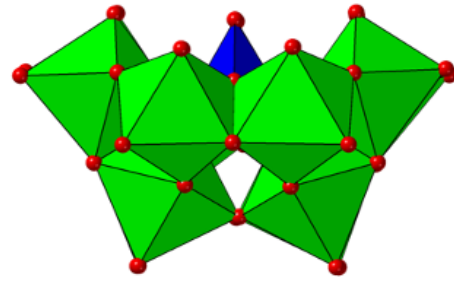
viewed along belt   viewed along cap

Figure S2. Polyhedral models of $[\gamma\text{-}P_2W_{12}O_{48}]^{14-}$. Color code: green, W; blue, P; red, O.
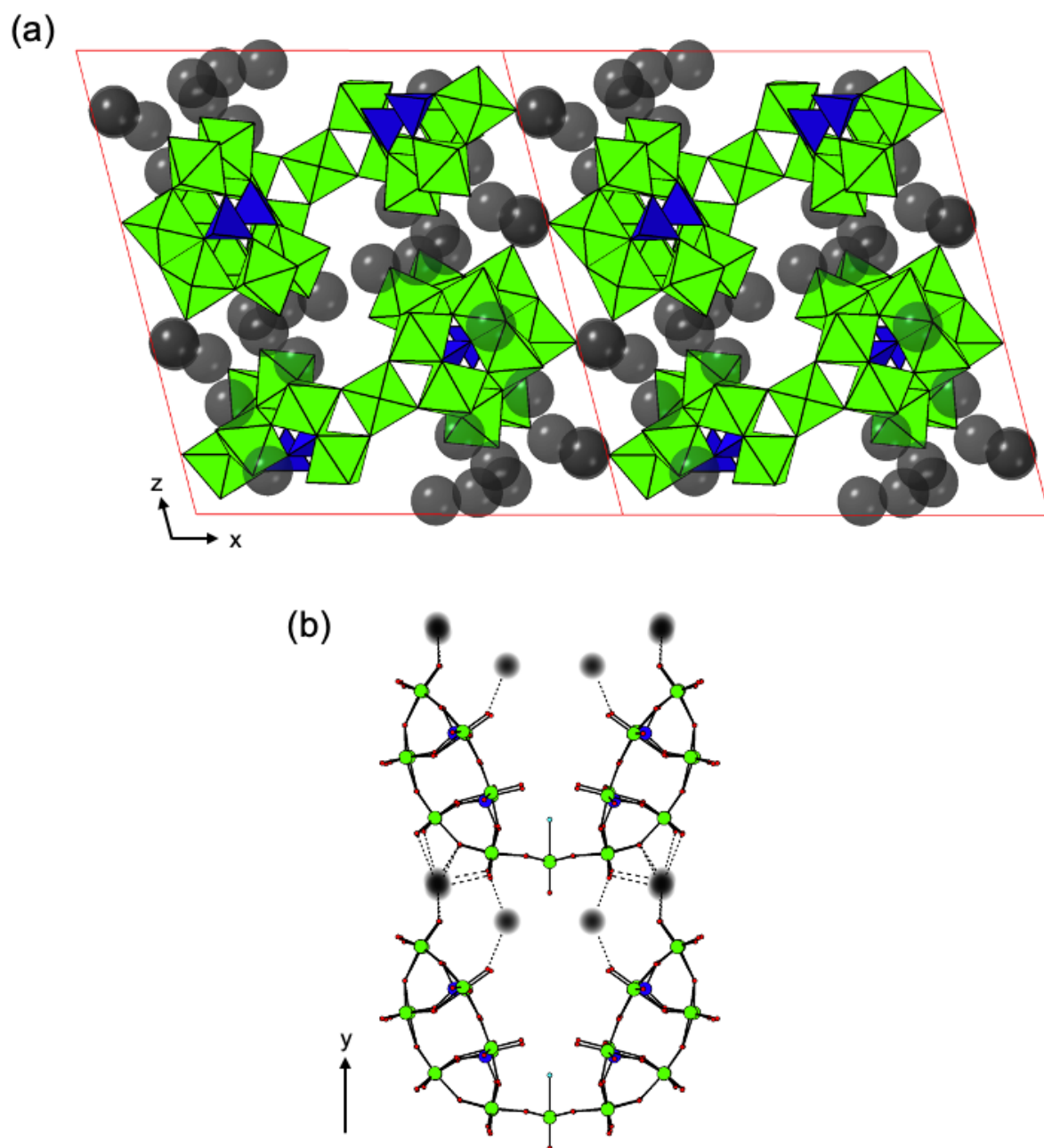
Figure S3. (a) Crystal packing of **2** with exterior K^+ counter cations shown and (b) part of the crystal packing illustrating stacking of $\{P_4W_{25}\}$ anions along the *b* direction. Color code: green, W; blue, P; red, O; cyan, aquo ligands; black, K.
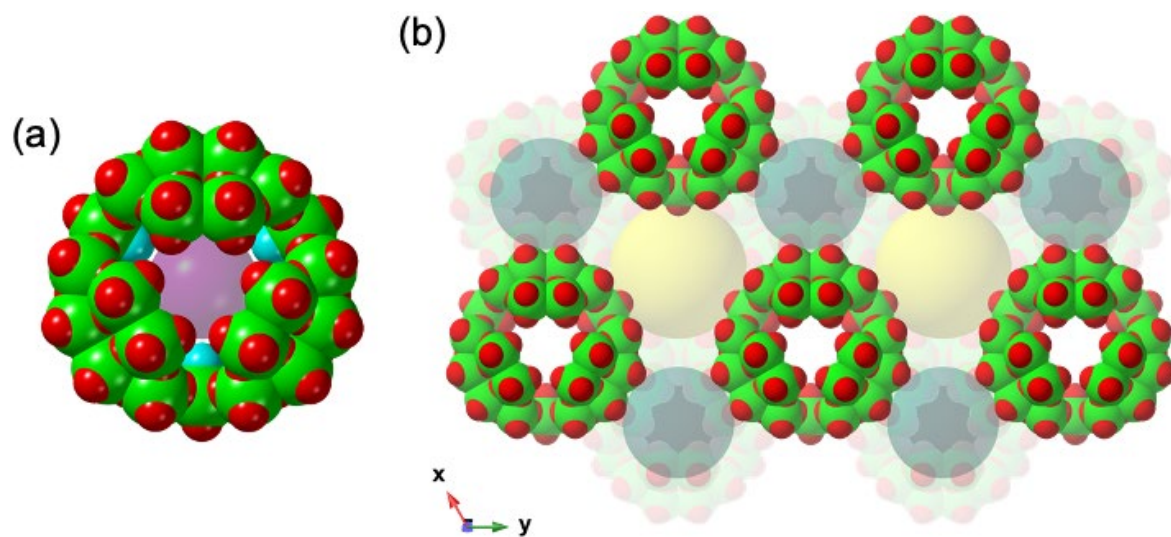
Figure S4. (a) A space-filling model of $\{P_6W_{39}\}$ showing (a) cluster's cavity emphasized by magenta sphere and (b) crystal packing of **3** with cavities represented by yellow (radius 7.7 Å) and deep cyan (radius = 6.3 Å) spheres.
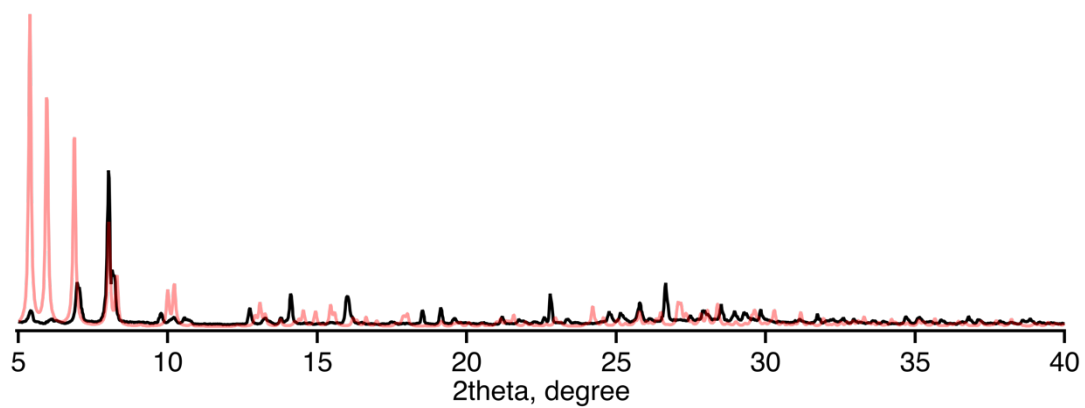
Figure S5. A room-temperature powder X-ray diffraction pattern of **3**. Black and red lines represent observed pattern and simulated pattern using single crystal structure, respectively.
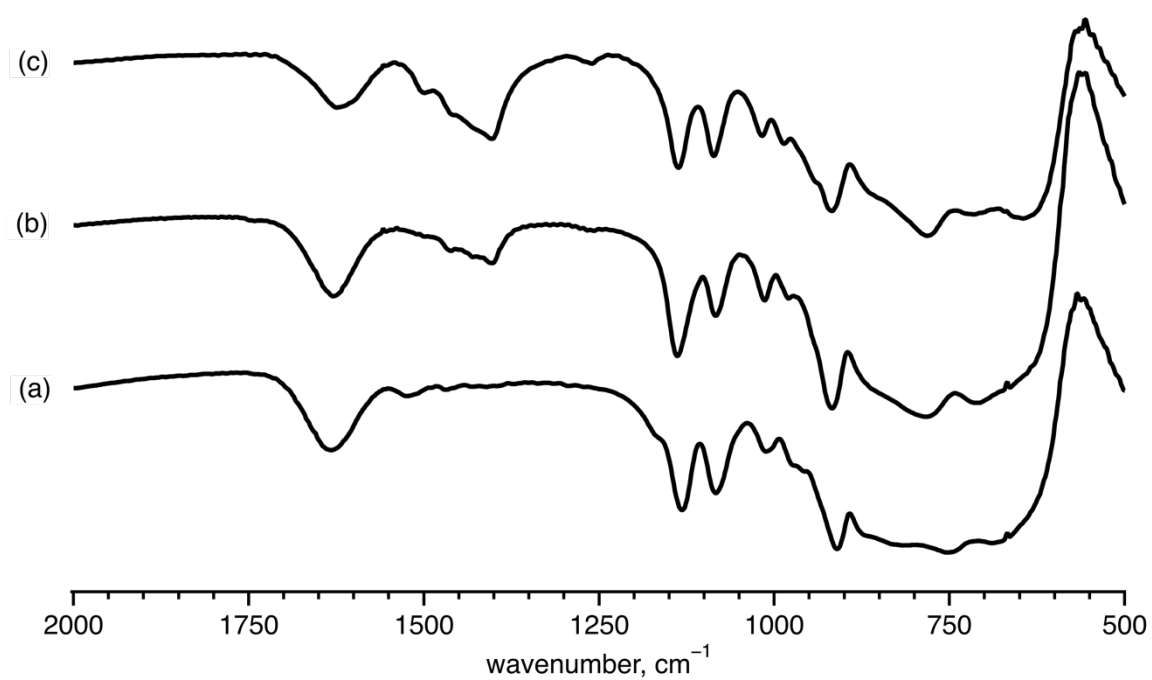
Figure S6. Fourier transform infrared spectra of (a) **1**, (b) **2**, and (c) **3**.
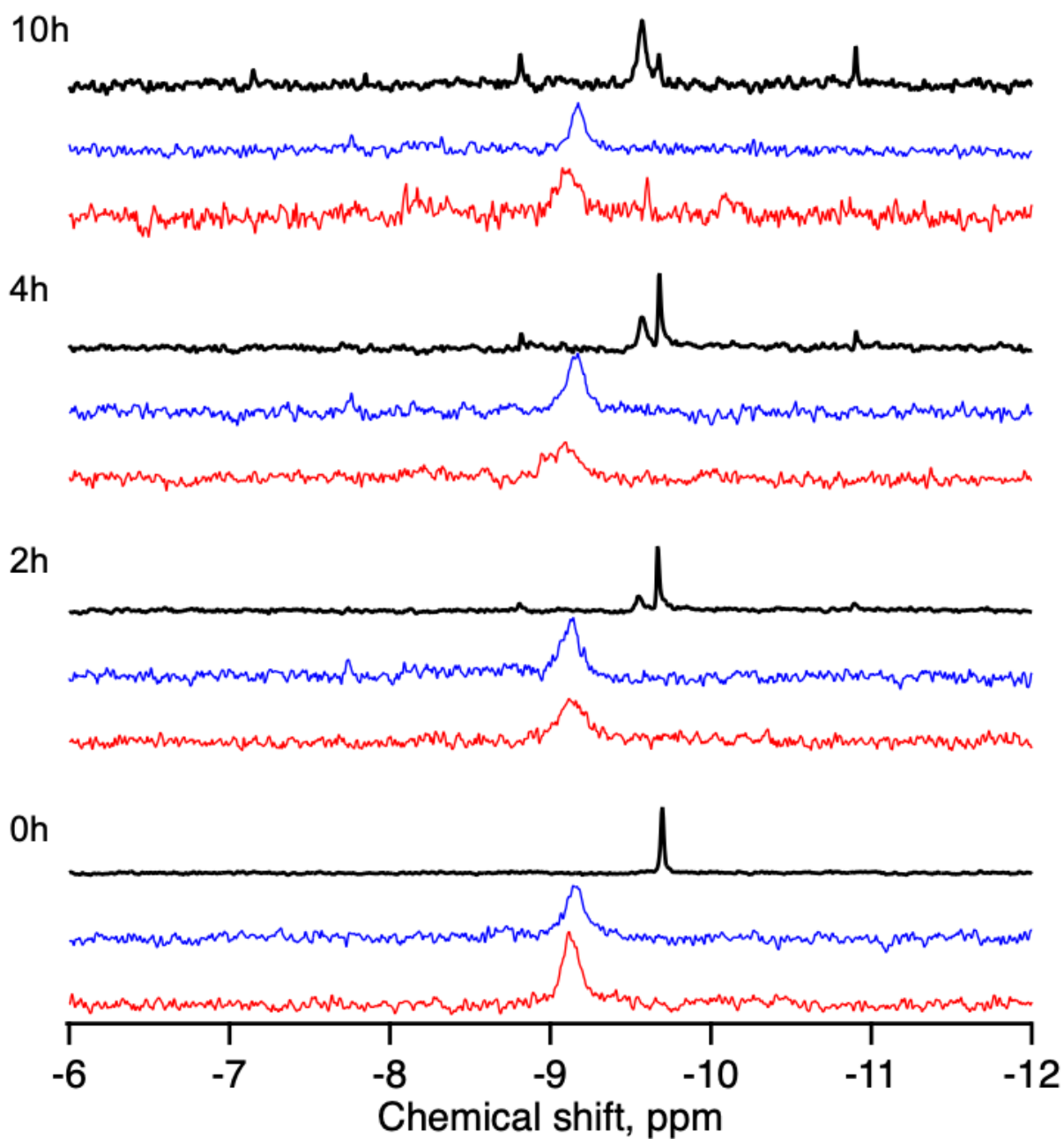
Figure S7. Time-dependent ^{31}P NMR spectra of **1** (red traces) and **2** (blue traces) in comparison with **3** (black traces).
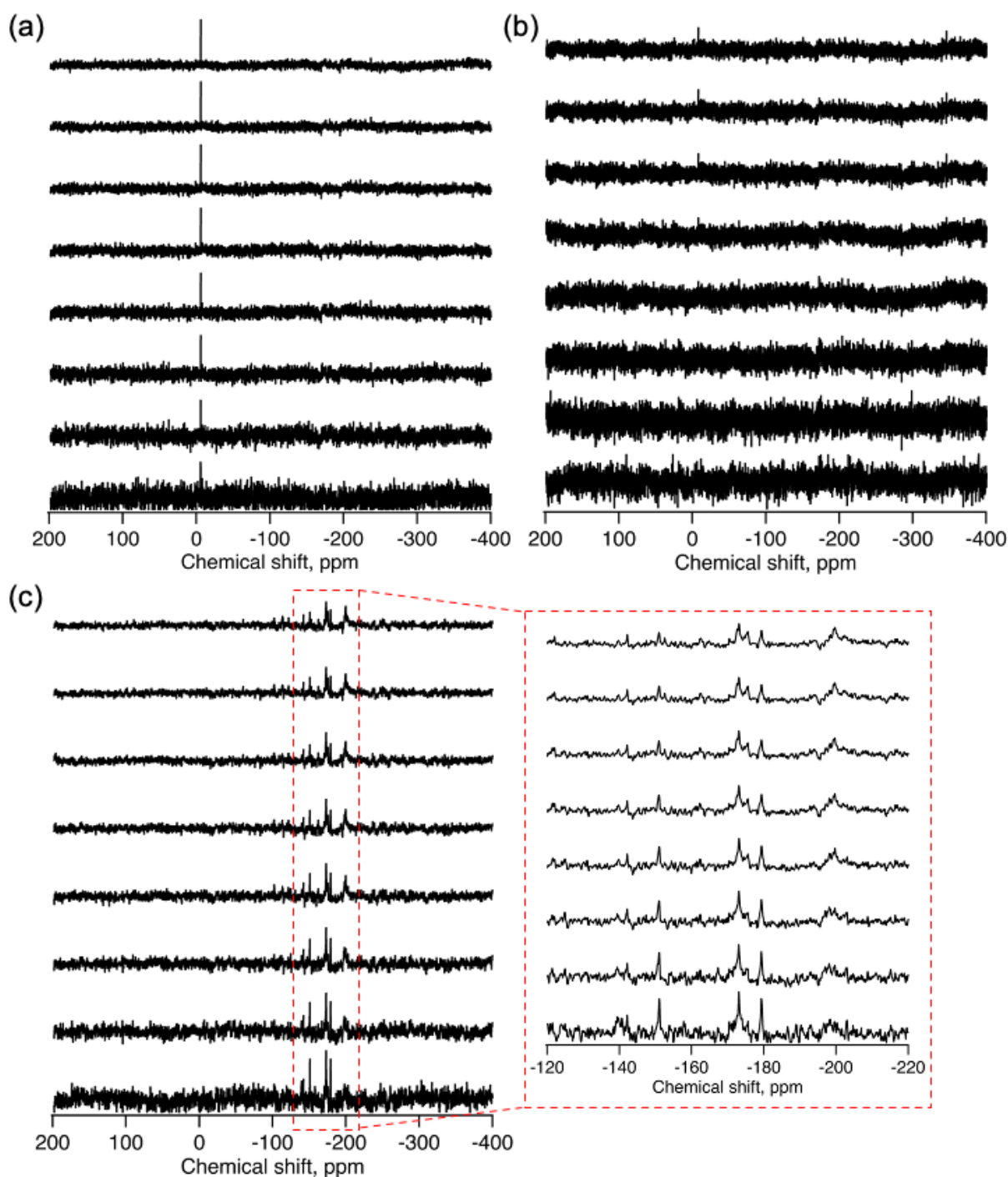
Figure S8. ^{183}W NMR spectra of (a) **1**, (b) **2**, and (c) **3** with magnified area between −120 and −220 ppm shown inside the dashed box. For each solution, 8 spectra were recorded every 1000, 2000, 3000, 4000, 5000, 6000, 7000, and 8000 scan numbers, and they were stacked from the bottom to the top traces, respectively; under our data collection setup, 1000 scan numbers correspond to approximately 2 hours. If {P$_2$W$_{12}$}, {P$_4$W$_{25}$}, and {P$_6$W$_{39}$} anions were stable in the solution, their ^{183}W NMR spectrum must show 3, 7, and 4 singlets, respectively. The ^{183}W NMR spectra of {P$_2$W$_{12}$} (**1**, panel a) showed only one singlet around 0 ppm corresponding to the decomposed [WO$_4$]$^{2-}$, whereas the ^{183}W NMR spectra of {P$_4$W$_{25}$}, (**2**, panel b) showed no clear signals. In the case of {P$_6$W$_{39}$}, (**3**, panel c), more than 5 ^{183}W NMR signals were observed.
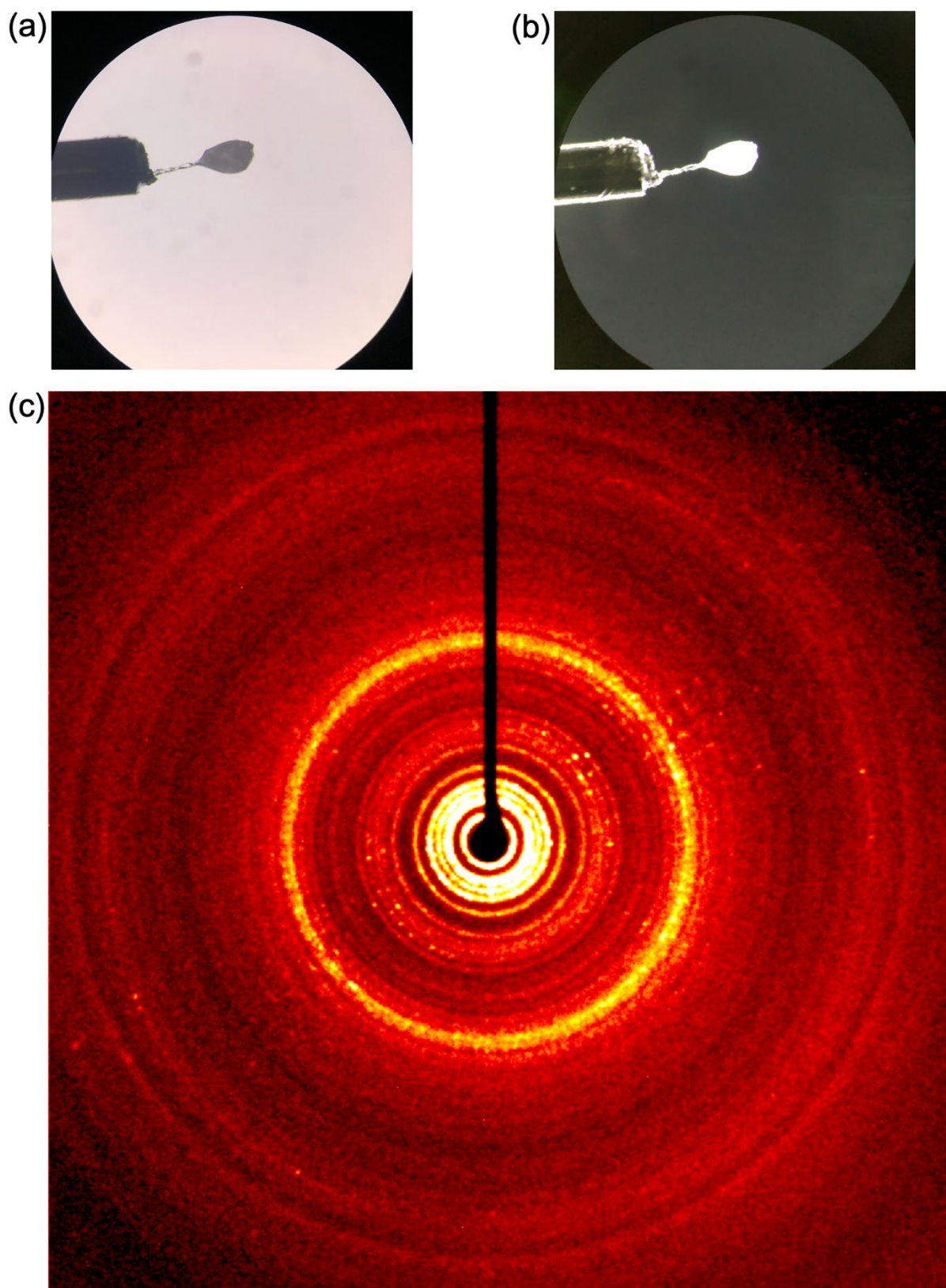
Figure S9. Microscope images of crystals of **3** mounted on a loop (diameter: 0.1 mm) taken under (a) bright field and (b) dark field and (c) the obtained diffraction rings. The black line is the shadow of the beamstop.
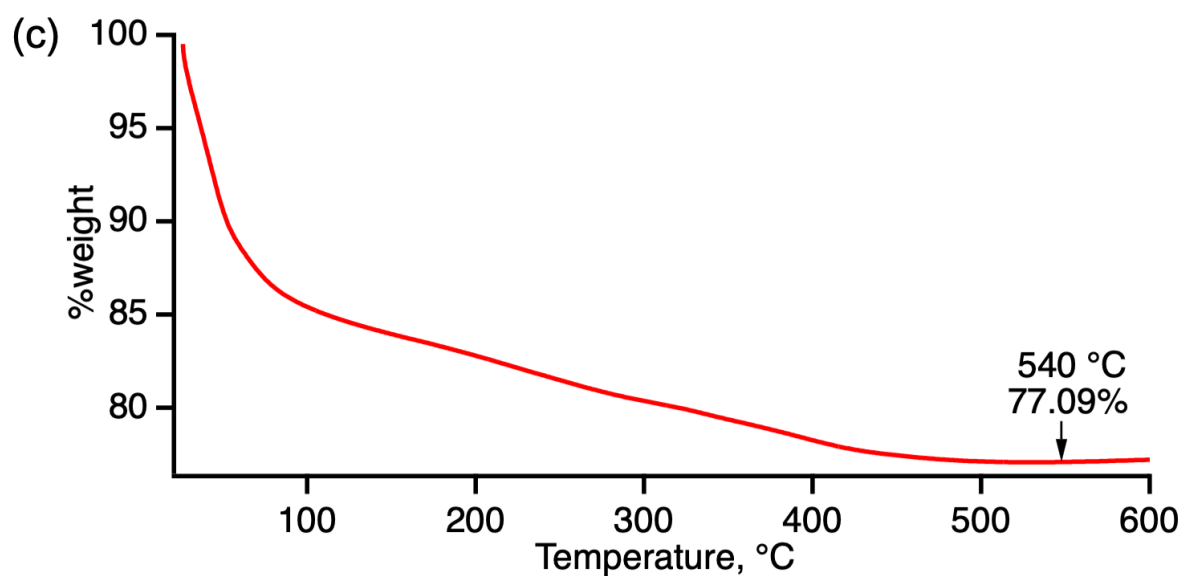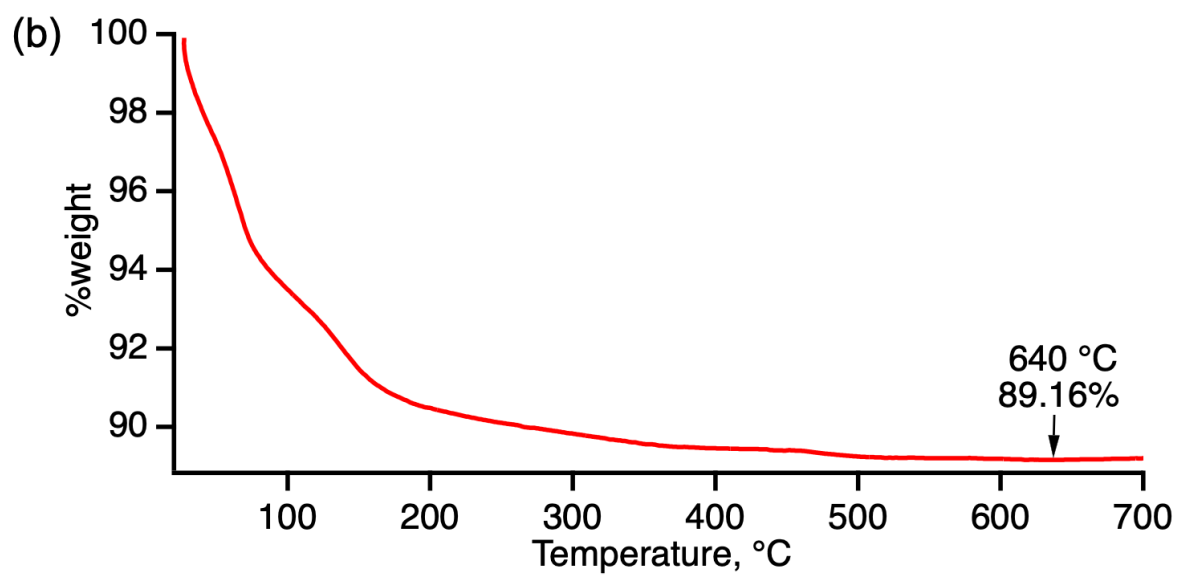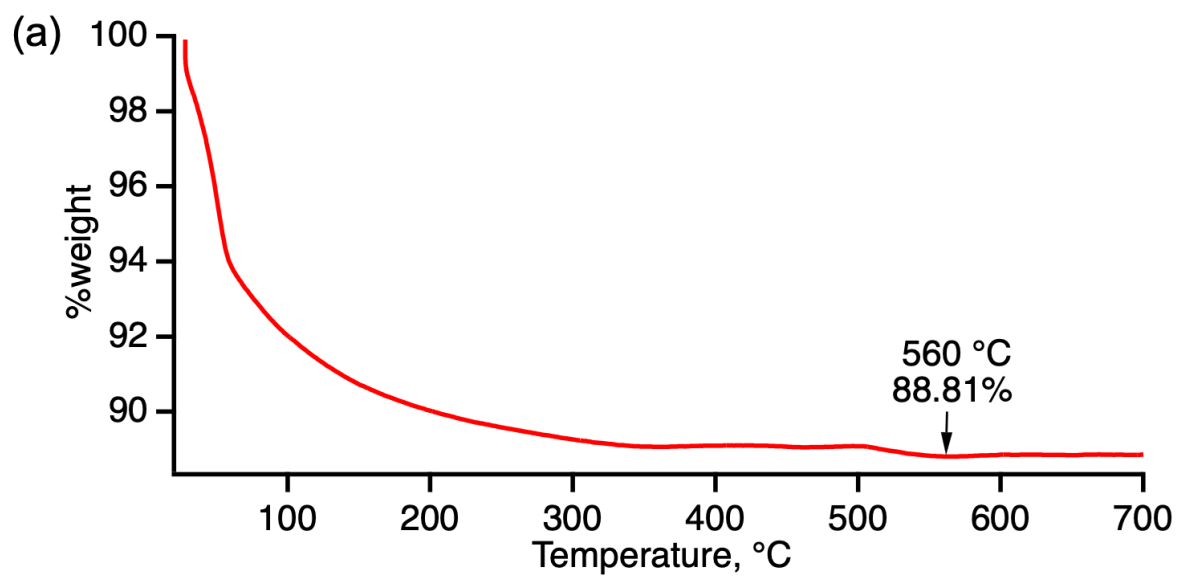
Figure S10. Thermograms of (a) **1**, (b) **2**, and (**3**).